European Journal of Operational Research xxx (xxxx) xxx

Contents lists available at ScienceDirect

European Journal of Operational Research

journal homepage: www.elsevier.com/locate/eor

Innovative applications of O.R.

Strategic flood impact mitigation in developing countries' urban road networks: Application to Hanoi

Siao-Leu Phouratsamay [a], Maria Paola Scaparra [b,*], Trung Hieu Tran [c], Gilbert Laporte [d,e]

[a] Univ. Grenoble Alpes, CNRS, Grenoble INP, G-SCOP, 38000 Grenoble, France
[b] Centre for Logistics and Sustainability Analytics, Kent Business School, University of Kent, Canterbury CT2 7PE, United Kingdom
[c] Centre for Design Engineering, Cranfield University, Cranfield MK43 0AL, United Kingdom
[d] HEC Montréal, Montréal, H3T 2A7, Canada
[e] School of Management, University of Bath, Bath, BA2 7AY, United Kingdom

ARTICLE INFO

Keywords:
OR in disaster relief
Flood mitigation
Optimization
Planning

ABSTRACT

Due to climate change, the frequency and scale of flood events worldwide are increasing dramatically. Flood impacts are especially acute in developing countries, where they often revert years of progress in sustainable development and poverty reduction. This paper introduces an optimization-based decision support tool for selecting cost-efficient flood mitigation investments in developing countries' urban areas. The core of the tool is a scenario-based, multi-period, bi-objective Mixed Integer Linear Programming model which minimizes infrastructure damage and traffic congestion in urban road networks. The tool was developed in collaboration with Vietnamese stakeholders (e.g., local communities and government authorities), and integrates data and inputs from other disciplines, including social science, transport economics, climatology and hydrology. A metaheuristic, combining a Greedy Randomized Adaptive Search Procedure with a Variable Neighborhood Descent algorithm, is developed to solve large scale problem instances. An extensive computational campaign on randomly generated instances demonstrates the efficiency of the metaheuristic in solving realistic problems with hundreds of interdependent flood mitigation interventions. Finally, the applicability of the interdisciplinary approach is demonstrated on a real case study to generate a 20-year plan of mitigation investments for the urban area of Hanoi. Policy implications and impacts of the study are also discussed.

1. Introduction

Floods are the most frequent disaster type, accounting for about 44% of all disaster events registered in the first two decades of this century, and affect the largest number of people worldwide (UNDRR, 2020). Recent studies found that almost a quarter of the world's population is directly exposed to high intensity floods (Rentschler et al., 2022) and that climate change projections indicate that the proportion of exposed population will increase further (Tellman et al., 2021). From 2000 to 2022, the Emergency Events Database (EM-DAT) recorded 3852 flood events worldwide affecting almost 1.8 billion people and causing 929 billion U.S. dollars of damage (CRED, 2023). Around 40% of these events occurred in Asia, making it the continent with the highest flood occurrence and highest flood economic impacts (ADRC, 2022).

Among Asian countries, Vietnam is one of the most prone to riverine and coastal flooding, due to its extended coastal areas, river basins and lakeshores (GFDRR, 2015). With 45.5 million people exposed to significant flood risks, Vietnam ranks third globally among countries with the highest flood exposure rate (Rentschler et al., 2022). Vietnamese cities experience severe floods every year, causing significant properties and public infrastructure damage, loss of business and livelihood options, contamination of water, and increase in water-related diseases. With rising temperatures and rainfall intensification due to climate change, in addition to changes in land-use patterns, rapid urbanization and acceleration in population growth, the frequency and severity of floods in Vietnam are expected to increase even further in the future (Huong & Pathirana, 2013; Rentschler et al., 2020).

As in many other countries facing similar flood disasters, flood impacts in Vietnamese cities affects overwhelmingly the poorest segments of society, who are more vulnerable to income losses and increased food prices during floods, have little resources for protecting their houses and other properties, and are less able to recover from property damage (Bangalore et al., 2019; Narloch & Bangalore, 2018; Rentschler et al., 2022). Investments in disaster mitigation measures can be particularly effective to prevent or mitigate the impact of flood

* Corresponding author.
E-mail address: m.p.scaparra@kent.ac.uk (M.P. Scaparra).

https://doi.org/10.1016/j.ejor.2024.06.035
Received 21 November 2023; Accepted 24 June 2024
Available online 26 June 2024

disasters given that flooding, unlike other disaster types, has affordable prevention mechanisms, including drainage systems, dykes, dams and early warning systems.

This paper presents the method and findings of an interdisciplinary study aiming at mitigating the negative social and economic impacts of urban floods in Vietnam through the identification of cost-efficient, long-term investments in structural flood protection measures. The study, conducted in collaboration with Vietnamese stakeholders in government and academia, and with the involvement of local communities, blends methods from different disciplines to develop an optimization model that determines the schedule of flood protection interventions minimizing road infrastructure damage and congestion in different flood scenarios.

The objectives of the model are determined based on the results of a socio-economic impact assessment, carried out with local communities in the central districts of Hanoi, Vietnam. The results of the impact assessment show that infrastructure damage and traffic congestion are the major concerns among the residents of Hanoi. As noted in the literature, societal flood impacts, both direct (e.g., property and infrastructure damage) and indirect (e.g., traffic disruptions and delays), are becoming more severe due to the increasing concentration of people and economic assets in flood prone areas and the greater frequency of flood events (Bubeck et al., 2017; Kefi et al., 2018). The community-based impact assessment confirmed these literature findings and revealed that the greatest social and economic flood impacts perceived by local communities are associated with road congestion and damage (Scaparra et al., 2019). The assessment also highlighted that the aging drainage system is considered to be the main cause of flooding in the city. The study thus considers a set of mitigation projects on the drainage system to minimize flood impacts on damage and congestion. The projects differ in terms of costs and impact reduction and a limited budget is available to implement them over a discrete planning horizon. A list of potential mitigation projects for Hanoi was compiled with the help of transport and drainage system experts, so as to test the model on a real case study.

To capture the uncertainty of future floods' intensity, the model considers different flood scenarios, evaluated in terms of flooding depth for events with different return periods, defined as the estimated time interval between two flood events of a similar intensity (Gumbel, 1941). Water depths for flood events of specific return periods can be computed using hydrological models, which combine topological maps, precipitation data, and drainage system data to produce flood maps. Heavy rainfall simulation and hydrological models were used by a team of climatologists and hydrologists to generate flood maps for the city of Hanoi in different climate change scenarios and estimate the benefit of the mitigation measures, in terms of water depth reduction (Dang et al., 2019).

The resulting Flood Mitigation Planning (FMP) problem, integrating all the above aspects, is formulated as a scenario-based, multi-period, bi-objective Mixed Integer Linear Programming (MILP) model. To capture the bi-objective nature of this complex problem, a simple weighted sum scalarization method is used. This has the advantage of turning the model into a single objective model that can then be solved by commercial optimization solvers. By suitably varying the weights, the supported non-dominated points on the Pareto front can be generated, providing the stakeholders with a reasonably-sized subset of trade-off solutions. Solving each instance of the single objective problem with general purpose solvers, however, becomes impractical for real-size problems. To overcome this, an ad hoc hybridization of a Greedy Randomized Adaptive Search Procedure (GRASP) (Feo & Resende, 1995) and a Variable Neighborhood Descent (VND) algorithm (Hansen & Mladenović, 1999) is developed and embedded into a Decision Support System (DSS) which enables city planners and policy makers to use the optimization tool and visualize the optimal mitigation measures and their impacts on a map. The GRASP-VND algorithm is validated and tested on randomly generated instances. The proposed approach is then used empirically for investigating cost effective ways in which flood road damage and congestion can be mitigated in Hanoi.

This study makes the following main scientific contributions: it introduces a new realistic flood mitigation optimization model co-designed with stakeholders and considering both direct and indirect flood impacts; it uses a unique confluence of distinct disciplines to generate primary data, define model inputs and identify key objectives; it proposes an ad hoc algorithm to solve the resulting complex model; it provides a real application and practical insights for the city of Hanoi; it develops a methodological framework general in scope and adaptable to other regions; it draws the attention of policy makers in Southeast Asia developing countries on the benefits of using analytic tools for decision making, thus serving as a catalyst for future projects.

The remainder of the paper is organized as follows. A literature review on optimization for flood mitigation and flood impact assessment is provided in Section 2. Section 3 provides an overview of the interdisciplinary modeling framework. The model assumptions and the FMP mathematical formulation are described in Section 4. The details of the hybrid GRASP-VND metaheuristic are given in Section 5. An experimental analysis is performed in Section 6. The results of the Hanoi case study are presented in Section 7. Finally, conclusive remarks and an outline of future research directions are given in Section 8.

2. Literature review and related works

Our work is rooted in two main streams of literature: flood mitigation optimization and flood impact assessment.

2.1. Optimization for flood mitigation

Optimization modeling has been applied to disaster operation management (DOM) since the early 1980s (Altay & Green, 2006). The DOM lifecycle includes four main programmatic phases: mitigation, preparedness, response and recovery (Altay & Green, 2006; Van Wassenhove & Pedraza Martinez, 2012). The mitigation phase includes actions taken to prevent disasters or reduce their impacts (e.g., risk assessments, facility protection, land use control). The preparedness phase spans planning, training and educational activities which prepare communities to respond to an emergency (e.g., pre-positioning of relief supplies, development of communication systems, response personnel training). The response phase is concerned with short-term critical actions taken in the aftermath of a disaster to save lives, including relief supply distribution, evacuation, emergency rescue and medical care. The recovery phase involves long-term post-disaster actions to restore normalcy, such as debris removal, buildings reconstruction, and infrastructure repair.

Optimization techniques have been used to tackle problems in all four phases, as documented in numerous survey papers (Altay & Green, 2006; Amideo et al., 2019; Besiou et al., 2018; Çelik et al., 2012; Çoban et al., 2021; Galindo & Batta, 2013; Grass & Fischer, 2016; Gupta et al., 2016; Özdamar & Ertem, 2015). In spite of this large body of literature, there are still several limitations to the applicability of DOM optimization models in practice. As noted in the reviews by Altay and Green (2006) and Galindo and Batta (2013), existent Operations Research (OR) works for disaster management are mostly model-driven rather than application-oriented. Several factors contribute to the scarcity of real applications. These include: lack of stakeholder engagement in the modeling process (Amideo et al., 2019; Galindo & Batta, 2013; Özdamar & Ertem, 2015), lack of interdisciplinary approaches and combination of different methodologies (Hoyos et al., 2015), unclear or unrealistic assumptions about some modeling aspects (Amideo et al., 2019; Galindo & Batta, 2013), scarce use of primary data and low data quality (Besiou et al., 2018; Gupta et al., 2016), limited understanding of specific disaster-related features (Çoban et al., 2021; Hoyos et al., 2015), and insufficient combination of practitioner and academic best practices (Özdamar & Ertem, 2015). A few surveys also advocate the

need to develop more complex models, including multi-objective and multi-period models (Caunhye et al., 2012; Gutjahr & Nolz, 2016; Hoyos et al., 2015), ad hoc cutting edge algorithms (Caunhye et al., 2012) and user-friendly interfaces to facilitate model uptake and implementation (Hoyos et al., 2015; Özdamar & Ertem, 2015). Finally, Gupta et al. (2016) point out that there is a lack of studies on specific types of disasters, including floods, and that more attention should be paid to the development of mitigation and prevention strategies against natural disasters.

Mitigation models have been widely studied over the past decades, especially within the context of facility protection in infrastructure networks and disruption risk mitigation in supply chains (see for example Bhuiyan et al. (2020), Gao et al. (2019), Hien et al. (2020), Starita and Scaparra (2021) for recent studies on these topics). However, the literature on optimization modeling for flood disaster mitigation is still quite sparse. Existent studies mostly focus on the problem of improving road networks against floods by strengthening or protecting infrastructure components. For example, Sohn (2006) proposes a link accessibility index based on distance and traffic flow to quantify the potential impact of flood damage and prioritize network links to retrofit in highway networks. Starita et al. (2017) propose a mixed-integer optimization model to determine optimal protection investments over a discrete planning horizon so as to minimize the expected shortest paths in road networks under different flood scenarios. Amin et al. (2020) consider the problem of determining optimal maintenance and rehabilitation operations as a mitigation measure to reduce the damage caused by floods on pavement roads in Bangladesh.

Another line of research, spurred by the 1953 flood in the Netherlands, specifically focuses on dikes as a mitigation measure against sea level rise and floods in delta regions. The first mathematical model to determine the optimal height of dikes is due to van Dantzig (1956). The findings of this cost–benefit model were incorporated in the Dutch Water Act and used to set up flood protection standards in the Netherlands. Brekelmans et al. (2012) propose an extension of the dike height optimization problem to the case of nonhomogeneous dike rings. Eijgenraam et al. (2017, 2014) improve previous dike upgrading models by incorporating the dynamic effects of climate change and socioeconomic growth in the cost–benefit analysis. Zwaneveld et al. (2018) further refine previous cost–benefit models by proposing an integer linear programming formulation to determine optimal timing and extent of dike heightening and strengthening. Finally, Postek et al. (2019) develop a robust optimization model to incorporate parameter uncertainty and decision adjustability in the design of flood risk management strategies based on dike heightening.

In summary, previous work on flood mitigation optimization has focused on road improvement or dike height optimization. In contrast, our paper considers improvements to drainage systems to reduce flood impacts on damage and congestion. As noted by Suarez et al. (2005), traffic congestion due to floods has significant negative impacts on transportation and livelihoods. However, congestion as a criterion to drive flood mitigation decisions has so far been neglected in existent studies on flood mitigation optimization. Our work also fills several of the gaps identified by recent DOM literature surveys by proposing a flood mitigation planning model, which is co-developed with government stakeholders and local communities, uses realistic and flood-disaster specific assumptions and data, and is based on inputs generated through the application of methodologies from other disciplines.

2.2. Flood impact assessment

Understanding and assessing potential impacts of flood events are critical components of flood risk management (Huizinga et al., 2017). Depending on whether the impacts can be quantified in monetary terms or not, flood damages are typically classified as tangible (e.g., property damage, business profit losses) and intangible (e.g., fatalities, health impacts, environmental losses) (Bubeck et al., 2017). Tangible damage can be further categorized in direct and indirect damage. Direct damage is caused by the direct contact with flood waters, whereas indirect damage is caused by the disruption of wider physical or economic systems and includes, for example, economic losses of suppliers, traffic disruptions and cascading impacts on interdependent infrastructure systems (Hammond et al., 2015).

Estimating direct flood damage is commonly done using stage-damage or depth-damage curves, which relate the expected damage of different property classes or infrastructure assets to the flood characteristics (e.g., water depth, duration and velocity). For example, Dutta et al. (2003) use stage-damage curves to estimate urban, rural and infrastructure losses in a river basin in Japan. Jonkman and Vrijling (2008) provide a function which correlates the flood depth to the mortality rate. Tariq et al. (2014) embeds stage-damage curves into a risk-based assessment approach to estimate flood insurance in the Chenab River region in Pakistan. Win et al. (2018) develop stage-damage functions to estimate house damage, in-house damage, income loss and agricultural damage in the Bago River Basin in Myanmar. Kefi et al. (2018) evaluate the tangible damage caused by floods in the urban area of To Lich river in Hanoi city.

Stage-damage functions have been mostly applied to evaluate direct tangible damages, principally on residential and commercial properties. In contrast, the understanding of indirect tangible damages and intangible damages, especially within the context of infrastructure systems, is still far from maturation (Hammond et al., 2015). As an example, the relation between flood events and their impacts on congestion and road traffic disruption has received little attention (Pyatkova et al., 2019). Systematic reviews highlighting the gaps in modeling the impacts of disaster events on transport disruption can be found in Faturechi and Miller-Hooks (2015) and Pregnolato et al. (2017). Pregnolato et al. (2017) are the first authors to propose a function which links flood depths to traffic speed, to estimate flood induced delays. The proposed depth-disruption function, derived by using video analysis and quantitative data from previous studies, is tested on the flood event of June 2012 in Newcastle upon Tyne, UK. This curve represents a breakthrough in modeling flood disruption in road networks as it overcomes a major limitation of previous approaches which consider roads either fully operational or fully blocked. A similar depth-disruption function is used by Choo et al. (2020) in combination with a rainfall-depth curve to create traffic disruption maps for the city of Seoul, Korea.

A widely used tool to evaluate congestion and traffic delays on roads is the Bureau of Public Roads (BPR) function, which relates travel times to traffic volumes (United States Bureau of Public Roads, 1964). Li et al. (2018) embeds the BPR model into a simulation tool to evaluate the impact of low returning frequency floods on traffic delays in Shanghai.

As described in Section 4, in our model we consider both direct tangible impacts on infrastructure, using a depth-damage curve similar to the one in Kefi et al. (2018), and the indirect damage associated with traffic congestion, using an adapted BPR function.

3. Interdisciplinary modeling framework

The development of the optimization-based flood mitigation decision support tool required an interdisciplinary approach integrating OR with other disciplines, including social science, transport economics, climatology, and hydrology. The overall methodology comprises five interrelated components, as displayed in Fig. 1.

In the first component, an impact assessment in selected hotspots of Hanoi was carried out in collaboration with social scientists at the Asian Management and Development Institute (AMDI) to identify the main perceived causes of floods in the city and the main flood-related concerns of local communities. The assessment involved about 500 participants, including residents and visitors (e.g. street vendors and taxi drivers). It revealed that improving drainage systems is the main priority for communities to reduce flood risk. It also highlighted that

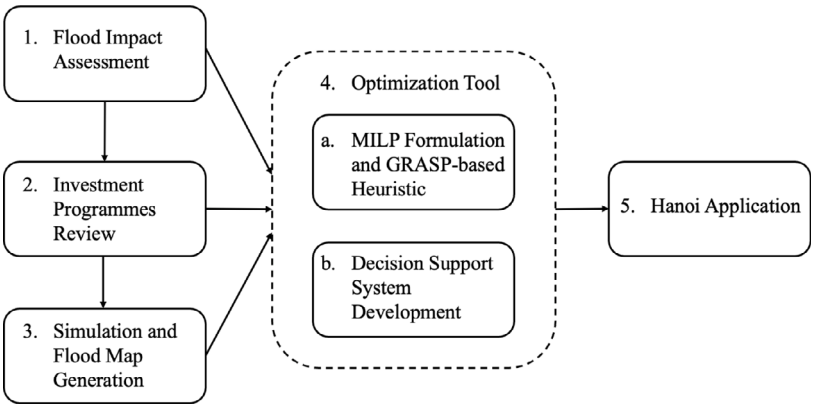

Fig. 1. The five components of our decision support tool.

the impacts of urban flooding are felt most acutely, and have the greatest economic and social impacts, along roads. Prolonged traffic congestion and children's absence from school were found to be the most important social impacts among residents. Overall, the assessment highlighted that road damage and traffic congestion were the major concerns among residents, street vendors and drivers. It also revealed that local communities advocate the need for government to take responsible action by upgrading or reconstructing the relevant drainage system (Scaparra et al., 2019). These findings were fed into the design and analysis of the subsequent project components.

The second component, a review of investment programmes, was carried out in collaboration with transport economists at the Transport Development and Strategy Institute (TDSI), to find a list of relevant drainage flood mitigation measures. Various documents, including the Master Plan 2030–2050 on urban rainwater drainage and lake conservation in Hanoi, were examined to identify a list of potential projects (e.g., lake rehabilitation, construction of manholes, reservoir upgrade, etc.), together with their costs, structural details and locations.

The third component aimed at estimating the benefit of each mitigation measure by building a set of future flood scenarios for Hanoi. To this end, meteorologists at the Vietnam Academy of Science and Technology (VAST) used the Weather Research and Forecasting model to simulate heavy rainfall in Hanoi, using historical data of the 2008 extreme rainfall event and two return periods of 20 years and 100 years. These two return periods are commonly used in flood risk assessment to model flooding events which differ in terms of magnitude and frequency of occurrence: a flood event with a 100-year return period is typically more intense and severe compared to a flood with a 20-year return period, but has a lower probability of occurrence (1% chance in any given year against 5%). Based on the rain flows produced by VAST and a hydrological model to set up the water flow in the pipes of the current drainage system of Hanoi, a team of hydrologists at the Vietnam Institute of Meteorology, Hydrology and Climate Change (IMHEN) generated accurate flood maps of Hanoi using the Mike Urban model (the interested reader is referred to Dang et al. (2019) for detailed explanations on the flood map generation). Flood maps were produced for the two scenarios (20- and 100-year return periods) without any mitigation measure, as well as with each mitigation measure. Combinations of measures affecting the same catchments were also considered. The flood maps provide an accurate estimate of the water levels in each flood scenario, when mitigation measures (e.g., installing larger pipes) are incorporated into the hydrological model.

The core of the methodology is the optimization tool developed in the fourth component. Using the data and results from the previous components, a scenario-based, multi-period, bi-objective MILP model was developed to identify cost-efficient long-term mitigation investment plans, able to reduce the impacts of future floods on the urban road network. The model inputs include: water levels in future flood scenarios, roads and catchments in the study area, cost and location of mitigation measures, predicted flood variations associated with mitigation measures, and available budget. Based on the results of the impact assessment, the model aims at minimizing two criteria: infrastructure damage and traffic congestion due to floods.

The MILP model and the GRASP-VND metaheuristic devised to solve it were embedded into a Decision Support System, which was then used in the last component to generate plans of future flood mitigation interventions for Hanoi.

4. Flood mitigation planning problem

Our mathematical model for the FMP problem is based on the following assumptions.

- The urban area is divided into catchments based on topographic characteristics. Each network link belongs to a specific catchment.
- Each project (e.g., increasing the capacity of a reservoir) is implemented in a given catchment and has an impact only on that catchment and its links. This simplifying assumption is based on preliminary flood map generation results, which show that the impact of a project in other catchments is negligible compared to the impact in its own catchment.
- The impact of different projects in the same catchment is not additive. Therefore, for each scenario, a separate flood map must be generated for each combination of projects in the same catchment, so as to evaluate the benefit of that project combination.
- Based on the results of the socio-economic impact assessment, the model aims at minimizing road congestion and damage. Specifically, the model minimizes a weighted linear combination of normalized damage rate and congestion level. The two objectives are normalized with respect to the total damage and congestion without any mitigation project. This way, the objectives explicitly measure the percentage improvements over the current state, a meaningful measure for the decision makers. The choice of using a simple weighted-sum method was also motivated by the need of providing decision makers with an intuitive tool. By changing the weights, decision makers can evaluate a range of different solutions from which to choose the preferred one, supported by the solution visualization tool described in Section 7.3.
- Based on the simulated water depths used to generate the flood maps, the benefit of each project combination, including single projects, is computed as the variation of the catchment area flooded at a given water depth. This variation affects the damage rate in the catchment. The flood maps also provide the variation of the length of each link in the catchment which is flooded at a given water depth. This variation affects the congestion level on the link.
- A limited budget is available in each time period and any unused budget can be rolled over to the next time period.

- The cost of each project does not change over the planning horizon and the duration of a project implementation is negligible with respect to the length of the time periods. This implies that a project benefit occurs from the time period when the project implementation starts. The proposed model can be easily modified to relax this assumption.

In the following, we denote by $\mathcal{S}$ the set of flood scenarios, where each scenario s is defined by its return period, and by $\mathcal{W}$, indexed by w, the set of water levels (note that we use water levels and water depths interchangeably throughout the paper). $\mathcal{K}$ represents the set of catchments and $\mathcal{L}_k$ the set of links in catchment k. The set of all links is denoted by $\mathcal{L}$. Each link l is defined by its capacity C_l (PCU/h), traffic volume V_l (PCU/h), length D_l (km) and vehicle speed limit S_l (km/h), where PCU stands for Passengers Car Unit.

Let $\mathcal{P}$ be the set of projects, $\mathcal{P}_k$ the set of projects in catchment k, and $\mathcal{T}$ the set of discrete time periods, with $T = |\mathcal{T}|$. B_t is the available budget in each time period t. Each project has a cost c_p and its implementation induces a variation of the flooded area and the links' flooded length in the catchment where it is implemented. The flooded area (km^2) of catchment k at water depth w in flood scenario s at the beginning of the time horizon is denoted by A_{kws0}. Similarly, A_{lws0} denotes the flooded length (km) of link l at water level w in flood scenario s at the beginning of the time horizon. Let $\mathcal{Q}_k = \{\mathcal{G}_q : q = 1, \dots, |\mathcal{Q}_k|\}$ be the set of project combinations $\mathcal{G}_q$ associated with catchment k. We denote by I_k the set of indexes of the project combinations in $\mathcal{Q}_k$, by $I_{kp} = \{q : q = 1, \dots, |\mathcal{Q}_k|, p \in \mathcal{G}_q\}$ the set of indexes of the project combinations in $\mathcal{Q}_k$ which include project p, and by $I_{k\bar{q}} = \{q : q = 1, \dots, |\mathcal{Q}_k|, |\mathcal{G}_q| > |\mathcal{G}_{\bar{q}}|\}$ the set of indexes of the project combinations in $\mathcal{Q}_k$ which have a cardinality larger than the cardinality of $\mathcal{G}_{\bar{q}}$. For instance, if there are two projects p_1, p_2 that can be implemented in a catchment k, the possible project combinations are $\mathcal{G}_1 = \{p_1\}$, $\mathcal{G}_2 = \{p_2\}$ and $\mathcal{G}_3 = \{p_1, p_2\}$, $\mathcal{Q}_k = \{\mathcal{G}_1, \mathcal{G}_2, \mathcal{G}_3\}$ and $I_{k1} = \{1, 3\}$ (set of indexes of combinations including project p_1). Then, A_{kwsq} (resp. L_{lwsq}) represents the predicted flooded area of catchment k (resp. flooded length of link $l \in \mathcal{L}_k$) at water depth w in scenario s when the projects in $\mathcal{G}_q \in \mathcal{Q}_k$ are implemented.

To compute the damage, we use the Flood Depth Damage Function introduced by Kefi et al. (2018), which provides direct damage rates, DR_w, as a function of flood depth w as follows:

$$DR_w = \frac{1}{1 + \exp(-a - b \times w)}$$

where a, b are parameters which need to be calibrated according to the study area.

To compute the congestion level, we use the BPR congestion function provided by the United States Bureau of Public Roads (1964) linking the traffic volume and the travel time:

$$T_V = \left(1 + \alpha \left(\frac{V}{C}\right)^{\beta}\right) T_0$$

where T_V is the travel time at traffic flow V, T_0 is the free-flow travel time, C is the capacity and α, β are road network dependent parameters. Since roads may be inundated, in the model we use VS_w (km/h) to denote the estimated vehicle speed at a water level w.

Finally, the model uses the following decision variables. The binary variable x_{pt} is equal to one if project p is implemented in period t and zero otherwise. The binary variable z_{kqt}, associated with combination $\mathcal{G}_q \in \mathcal{Q}_k$, indicates whether combination $\mathcal{G}_q$ is active in period t. Namely, z_{kqt} takes value one if all the projects in combination $\mathcal{G}_q$ are implemented either in period t or before t, zero otherwise. Variable a_{kwst} (resp. ℓ_{lwst}) denotes the flooded area (resp. length) in m^2 (resp. km) of catchment k (resp. link l) with a water level w in flood scenario s in period t. Variable y_{st} defines the damage rate in scenario s in time period t. The congestion level (hours) of link l in flood scenario s in period t is denoted by u_{lst}. The free flow travel time (hours) of link l associated with water depth w in scenario s and in time period t is given by τ_{lwst}. The notation used throughout the paper is summarized in Table 1 of the supplementary material.

The FMP problem can be formulated as a MILP model as follows:

$$\text{minimize } z = \lambda \frac{z_1}{\bar{D}_B} + (1 - \lambda) \frac{z_2}{\bar{C}_B} \tag{1}$$

subject to

$$z_1 = \sum_{t \in \mathcal{T}} \delta_t \sum_{s \in \mathcal{S}} \beta_s y_{st}, \tag{2}$$

$$A_{kws0}(1 - \sum_{q \in I_k} z_{kqt}) + \sum_{q \in I_k} A_{kwsq} z_{kqt} \le a_{kwst}$$
$$\forall k \in \mathcal{K}, \forall w \in \mathcal{W}, \forall s \in \mathcal{S}, \forall t \in \mathcal{T}, \tag{3}$$

$$y_{st} = \sum_{k \in \mathcal{K}} \gamma_k \sum_{w \in \mathcal{W}} DR_w a_{kwst} \qquad \forall s \in \mathcal{S}, \forall t \in \mathcal{T}, \tag{4}$$

$$z_2 = \sum_{t \in \mathcal{T}} \delta_t \sum_{s \in \mathcal{S}} \beta_s \sum_{k \in \mathcal{K}} \gamma_k \sum_{l \in \mathcal{L}_k} u_{lst}, \tag{5}$$

$$L_{lws0}(1 - \sum_{q \in I_k} z_{kqt}) + \sum_{q \in I_k} L_{lwsq} z_{kqt} \le \ell_{lwst}$$
$$\forall k \in \mathcal{K}, \forall l \in \mathcal{L}_k, \forall w \in \mathcal{W}, \forall s \in \mathcal{S}, \forall t \in \mathcal{T}, \tag{6}$$

$$\tau_{lwst} \ge \ell_{lwst} / VS_w$$
$$\forall l \in \mathcal{L}, \forall w \in \mathcal{W}, \forall s \in \mathcal{S}, \forall t \in \mathcal{T}, \tag{7}$$

$$\tau_{l0st} \ge (D_l - \sum_{w \in \mathcal{W}} \ell_{lwst}) / S_l$$
$$\forall l \in \mathcal{L}, \forall s \in \mathcal{S}, \forall t \in \mathcal{T}, \tag{8}$$

$$u_{lst} = \left(1 + \alpha \left(\frac{V_l}{C_l}\right)^{\beta}\right) \sum_{w \in \mathcal{W} \cup \{0\}} \tau_{lwst} \qquad \forall l \in \mathcal{L}, \forall s \in \mathcal{S}, \forall t \in \mathcal{T}, \tag{9}$$

$$\sum_{t \in \mathcal{T}} x_{pt} \le 1 \qquad \forall p \in \mathcal{P}, \tag{10}$$

$$\sum_{q \in I_k} z_{kqt} \le 1 \qquad \forall k \in \mathcal{K}, \forall t \in \mathcal{T}, \tag{11}$$

$$x_{pt} \le \sum_{q \in I_{kp}} z_{kqt} \qquad \forall k \in \mathcal{K}, \forall p \in \mathcal{P}_k, \forall t \in \mathcal{T}, \tag{12}$$

$$|\mathcal{G}_q| z_{kqt} \le \sum_{j \le t} \sum_{p \in \mathcal{G}_q} x_{pj} \qquad \forall k \in \mathcal{K}, \forall t \in \mathcal{T}, \forall q \in I_k, \tag{13}$$

$$z_{k\bar{q}t} \le z_{k\bar{q}j} + \sum_{q \in I_{k\bar{q}}} z_{kqj} \qquad \forall k \in \mathcal{K}, \forall t \in \mathcal{T}, \forall j > t, \forall \bar{q} \in I_k, \tag{14}$$

$$(|\mathcal{G}_{\bar{q}}| + 1)(1 - z_{kqj}) + |\mathcal{G}_q| z_{kqj}$$
$$\ge (|\mathcal{G}_{\bar{q}}| + 1) z_{k\bar{q}t} \qquad \forall k \in \mathcal{K}, \forall t, j \in \mathcal{T} : j > t, \forall \bar{q}, q \in I_k : \bar{q} \ne q, \tag{15}$$

$$\sum_{j \le t} \sum_{p \in \mathcal{P}} c_p x_{pj} \le \sum_{j \le t} B_j \qquad \forall t \in \mathcal{T}, \tag{16}$$

$$x_{pt} \in \{0, 1\} \qquad \forall p \in \mathcal{P}, \forall t \in \mathcal{T}, \tag{17}$$

$$z_{kqt} \in \{0, 1\} \qquad \forall k \in \mathcal{K}, \forall q = 1, \dots, |\mathcal{Q}_k|, \forall t \in \mathcal{T}, \tag{18}$$

$$y_{st} \ge 0 \qquad \forall s \in \mathcal{S}, \forall t \in \mathcal{T}, \tag{19}$$

$$a_{kwst} \ge 0 \qquad \forall k \in \mathcal{K}, \forall w \in \mathcal{W}, \forall s \in \mathcal{S}, \forall t \in \mathcal{T}, \tag{20}$$

$$\ell_{lwst} \ge 0 \qquad \forall l \in \mathcal{L}, \forall w \in \mathcal{W}, \forall s \in \mathcal{S}, \forall t \in \mathcal{T}, \tag{21}$$

$$u_{lst} \ge 0 \qquad \forall l \in \mathcal{L}, \forall s \in \mathcal{S}, \forall t \in \mathcal{T}, \tag{22}$$

$$\tau_{lwst} \ge 0 \qquad \forall l \in \mathcal{L}, \forall w \in \mathcal{W} \cup \{0\}, \forall s \in \mathcal{S}, \forall t \in \mathcal{T}. \tag{23}$$

The objective function (1) minimizes a weighted linear combination of normalized damage and congestion, computed over different flood scenarios, catchments and time periods. In (1), λ is the objective weight, while $\bar{D}_B$ and $\bar{C}_B$ are constants denoting respectively the total damage rate and total congestion level at the beginning of the planning horizon (with no mitigation measures).

The damage function z_1 is computed by Constraints (2)–(4). Specifically, the flooded area a_{kwst} in catchment k at water level w in scenario s and in time period t is derived by Constraints (3), by taking into account the flooded area A_{kwsq} induced by the selected project combination in catchment k. This is then used in combination with the damage rate provided in Kefi et al. (2018) to compute the overall damage for a specific time period and scenario in Constraints (4). Finally, the overall damage across all scenarios and time periods is computed by Constraints (2). Note that to allow flexibility in the model, catchments, time periods and scenarios can have different weights (denoted by γ_k, δ_t and β_s respectively).

The congestion function z_2 is computed by Constraints (5)–(9). Similarly to Constraints (3), Constraints (6) define the flooded length ℓ_{lwst} of link l at water level w in scenario s and time period t. Flooded lengths are used to compute the free-flow travel time on flooded roads in Constraints (7) and the free-flow travel times on non-flooded roads in Constraints (8). Note that the value $(D_l - \sum_{w \in \mathcal{W}} \ell_{lwst})$ in Constraints (8) corresponds to the total non-flooded length of link l in scenario s and time period t. Constraints (9) compute the congestion levels u_{lst} using the BPR function (United States Bureau of Public Roads, 1964). Finally, the overall congestion across all links, scenarios and time periods is computed by Constraints (5).

Constraints (10) indicate that a project p can be implemented at most once over the planning horizon. Constraints (11) ensure that in a given period t, at most one combination of projects can be active in each catchment k. Constraints (12) guarantee that if a project p is implemented in period t, then one combination including project p has to be active in period t. Constraints (13) ensure that if a combination $\mathcal{G}_q$ in catchment k is active in period t ($z_{kqt} = 1$), then all projects $p \in \mathcal{G}_q$ have to be implemented either in period t or before period t. Constraints (14) indicate that if a combination $\mathcal{G}_{\bar{q}}$ is active in period t, then a combination in the same catchment has to be active in each subsequent period $j > t$. This can be the same combination or a combination with more projects than $\mathcal{G}_{\bar{q}}$. In a feasible solution, if a combination $\mathcal{G}_{\bar{q}}$ is active in period t, then only a combination $\mathcal{G}_q$ with more than $|\mathcal{G}_{\bar{q}}|$ projects can be active after period t. This is ensured by Constraints (15). Constraints (16) represent the budget limit in each time period. Constraints (17)–(23) define the domain of the variables.

5. A hybrid GRASP-VND metaheuristic

For a given choice of the objective weight λ, small and medium-sized instances of FMP can be solved using commercial optimization software. However, realistic instances may involve hundreds of potential interventions in many catchments and over long time horizons. Solving them by general purpose solvers is impractical, due to excessive computing time and memory requirements (see Section 6). In addition the stakeholders who commissioned the study required a solution approach not reliant on licensed software. We therefore developed a multi-start, two-phase GRASP-VND metaheuristic. In each start, GRASP, introduced by Feo and Resende (1995), is used in the constructive phase to build a feasible solution by randomly selecting promising elements from a dynamic Restricted Candidate List (RCL). The feasible solution is then improved using a VND algorithm (see Hansen & Mladenović, 1999), which systematically explores different neighborhoods within a local search. The algorithm stops if either a maximum number of iterations or a maximum computing time is reached.

5.1. Constructive phase

The constructive phase begins with an empty solution and iteratively adds a project to the solution following a randomized greedy procedure until no project can be added to the solution without exceeding the available budget. We denote by *plan* the partial solution built during the constructive phase. The randomized greedy procedure guides the construction of the solution using a greedy function defined by the benefit of adding a project into the partial solution. Let (t, p) be a couple representing a project p implemented in time period t.

We defined the greedy function ϕ_{tp} as:

$$\phi_{tp} = \frac{\lambda \Delta \text{Damage}_{tp} + (1-\lambda)\Delta \text{Congestion}_{tp}}{c_p} \tag{24}$$

where ΔDamage_{tp} and $\Delta\text{Congestion}_{tp}$ are the normalized damage and congestion variations induced by the implementation of project p in time period t. Note that if the partial solution *plan* includes other projects belonging to the same catchment as p and implemented before t, the damage and congestion variations in the greedy function are computed by activating and deactivating project combinations in that catchment accordingly.

At each iteration of the constructive phase, the RCL contains the best candidates to be inserted into the partial solution. It is constructed so that the couples (t, p), where project p is not implemented in the partial solution *plan* and t is the earliest time when p can be implemented depending on the available budget, are ranked using the greedy function (24). A couple (t, p) is inserted in the RCL if implementing project p at its earliest time period t is feasible, *i.e.* the budget constraint is not violated, and the greedy function ϕ_{tp} is in the interval $[\eta\phi_{\max}, \phi_{\max}]$ where $\phi_{\max}$ is the maximum value ϕ_{tp} of the potential couples (t, p) and η varies between 0 and 1. The selection of the parameter η to construct the RCL has an impact on the quality of the solution built in the constructive phase. In our experimentation we use a reactive GRASP (Prais & Ribeiro, 2000) to define the value of η at each iteration.

Once the RCL is constructed, a candidate $(\bar{t}, \bar{p})$ is randomly chosen from the RCL and added to the partial solution *plan*. The residual budget and greedy function for the remaining candidates are then updated accordingly. The constructive phase ends when no candidate project can be added to the partial solution without exceeding the available residual budget. The feasible solution is then improved through the local search phase.

5.2. Improvement phase

The VND search uses a set $\mathcal{N} = \{\mathcal{N}_1, \ldots, \mathcal{N}_5\}$ of five operators such that operator $\mathcal{N}_j$, $j = 1, \ldots, 5$, maps a given solution *plan* to a predefined neighborhood structure $\mathcal{N}_j(plan)$. The algorithm explores the neighborhood structures using a sequential neighborhood change step (Hansen et al., 2017), whereby if an improvement of the incumbent solution in some neighborhood structure occurs, the search is resumed in the first neighborhood structure $\mathcal{N}_1(plan)$ of the new incumbent solution; otherwise the search is continued in the next neighborhood, according to the order in $\mathcal{N}$. The exploration of each neighborhood uses a best improvement strategy. The VND algorithm starts with the solution returned by the constructive phase as the incumbent solution *plan* and terminates when no improving solution can be found in any of the neighborhood structures. The five operators can be classified into two types: *period operators* ($\mathcal{N}_1$, $\mathcal{N}_2$, and $\mathcal{N}_3$), which only change the implementation periods of the projects in the incumbent solution; and *project operators* ($\mathcal{N}_4$ and $\mathcal{N}_5$), which swap projects in the solution with projects not in the solution. Note that only operators which produce feasible solutions with respect to the budget constraints are attempted.

In the following, we denote by $\mathcal{P}^{in}$ the set of projects implemented in *plan* and by $\mathcal{P}^{out}$ the ones not implemented in *plan*. The set of projects in *plan* implemented in time period t is denoted by $\mathcal{P}^{in}_t$. The operators are defined as follows.

$\mathcal{N}_1$: **One-to-Many Period Operator.** Given a period $t \in \mathcal{T} \setminus \{T\}$ and a project $p \in \mathcal{P}^{in}_t$, this operator moves project p forward to a subsequent period $\bar{t}$, with $\bar{t} = t+1, \ldots,$ min $\{t+h, T\}$, for some $h \geq 1$. It then tries to move backward projects that are implemented in period $\bar{t}$ in the following way: for each project $\bar{p} \in \mathcal{P}^{in}_{\bar{t}}$, project $\bar{p}$ is moved backward from period $\bar{t}$ to its earliest feasible (with respect to the budget) implementation period, if it exists; then as many projects as possible following $\bar{p}$ in $\mathcal{P}^{in}_{\bar{t}}$ are moved from period $\bar{t}$ to their earliest

Table 1
Example of solutions generated by the One-to-Two Period operator.

(a) Incumbent solution

Period	$\mathcal{P}^{in}$				
1	p_1	p_2	p_3		
2	p_4	p_5			
3	p_6	p_7	p_8	p_9	
$\mathcal{P}^{out}$	p_{10}	p_{11}	p_{12}		

(b) Solution with $t = 1, \bar{t} = 3, p = p_1, \bar{p} = p_6$.

Period	$\mathcal{P}^{in}$		
1	p_2	p_3	$\boldsymbol{p_9}$
2	p_4	p_5	$\boldsymbol{p_6}$
3	p_7	p_8	$\boldsymbol{p_1}$
$\mathcal{P}^{out}$	p_{10}	p_{11}	p_{12}

(c) Solution with $t = 1, \bar{t} = 3, p = p_1, \bar{p} = p_7$.

Period	$\mathcal{P}^{in}$			
1	p_2	p_3	$\boldsymbol{p_7}$	
2	p_4	p_5	$\boldsymbol{p_8}$	$\boldsymbol{p_9}$
3	p_6	$\boldsymbol{p_1}$		
$\mathcal{P}^{out}$	p_{10}	p_{11}	p_{12}	

Table 2
Example of solution generated by the One-to-Many Two-Period operator.

(a) Incumbent solution

Period	$\mathcal{P}^{in}$			
1	p_1	p_2	p_3	
2	p_4	p_5		
3	p_6	p_7	p_8	p_9
$\mathcal{P}^{out}$	p_{10}	p_{11}	p_{12}	

(b) Solution after the operator

Period	$\mathcal{P}^{in}$			
1	p_1	p_3	$\boldsymbol{p_5}$	
2	p_4	$\boldsymbol{p_9}$		
3	p_6	p_7	p_8	$\boldsymbol{p_2}$
$\mathcal{P}^{out}$	p_{10}	p_{11}	p_{12}	

feasible implementation period. These projects are tried in the order of appearance in $\mathcal{P}^{in}_{\bar{t}}$.

Example. *Table 1 displays two solutions generated by the One-to-Many Period operator for a problem with 12 projects and 3 time periods. Table 1a shows the incumbent solution where* $\mathcal{P}^{in}_1 = \{p_1, p_2, p_3\}$, $\mathcal{P}^{in}_2 = \{p_4, p_5\}$ *and* $\mathcal{P}^{in}_3 = \{p_6, p_7, p_8, p_9\}$. *Tables 1b and 1c present two period exchanges for project* $p = p_1 \in \mathcal{P}^{in}_1$ *from its current implementation period* $t = 1$ *to period* $\bar{t} = 3$. *In Table 1b, the solution is obtained by moving project* $\bar{p} = p_6$ *backward to its earliest feasible period 2; then the projects following* p_6 *in* $\mathcal{P}^{in}_3$ *(i.e.,* p_7, p_8, p_9*) are considered and as many projects as possible are moved backward (in the example, only project* p_9 *is moved backward). In Table 1c, starting from the incumbent solution, project* $\bar{p} = p_7$ *is moved first to its earliest feasible period 1; then the set of projects following* p_7 *in* $\mathcal{P}^{in}_3$ *is considered (i.e.,* p_8, p_9*) and both projects* p_8 *and* p_9 *are moved backward to period 2.*

$\mathcal{N}_2$: **Two-to-Many Period Operator.** This operator is equivalent to the One-to-Many Period operator but instead of moving only one project to a later period, for each period $t \in \mathcal{T}\backslash\{T\}$, two projects $p, p' \in \mathcal{P}^{in}_t$ (if they exists) are moved forward to a subsequent period $\bar{t}$, with $\bar{t} = t+1, \ldots,$ min $\{t+h, T\}$, for some $h \geq 1$. Projects in $\mathcal{P}^{in}_{\bar{t}}$ are then moved backward as in $\mathcal{N}_1$.

$\mathcal{N}_3$: **One-to-Many Two-Period Operator.** Let $t \in \{1, \ldots, T-2\}$ and $\bar{t} \in \{t+2, t+3\}$ be two time periods. In this operator, a project $p \in \mathcal{P}^{in}_t$ is first moved forward from period t to period $\bar{t}$. Then, a project $\bar{p} \in \mathcal{P}^{in}_{\bar{t}-1}$, is moved backward from period $\bar{t}-1$ to its earliest feasible implementation period. Finally, as many projects $\tilde{p} \in \mathcal{P}^{in}_{\bar{t}}$ as possible are moved from period $\bar{t}$ to their earliest feasible implementation period. Namely, projects are moved backward from two different time periods ($\bar{t}-1$ and $\bar{t}$) rather than only one as in the previous operators.

Example. *Table 2 displays a solution generated by the One-to-Many Two-Period operator. Table 2a shows the incumbent solution. Table 2b shows the solution obtained by moving project* p_2 *forward from period* $t = 1$ *to period* $\bar{t} = 3$. *Then project* p_5 *is moved backward from period* $\bar{t}-1 = 2$ *to its earliest feasible period 1. Finally, project* p_9 *is moved backward from period* $\bar{t} = 3$ *to its earliest feasible implementation period 2.*

$\mathcal{N}_4$: **One-to-Many Project Operator.** Given a time period $t \in \mathcal{T}$ and a project $p \in \mathcal{P}^{in}_t$, p is removed from $\mathcal{P}^{in}_t$ and inserted into $\mathcal{P}^{out}$. Then as many projects as possible from $\mathcal{P}^{out}$ are added to the solution in their earliest feasible implementation period. Note that project p, once inserted in $\mathcal{P}^{out}$, can be selected to be added to the solution again but its implementation period can be different from the one in the initial solution.

$\mathcal{N}_5$: **Two-to-Many Project Operator.** This operator is equivalent to the One-to-Many Project Operator but instead of removing only one project from the incumbent solution, for each time period $t \in \mathcal{T}$, two projects p and p' are moved from P^{in}_t to P^{out}. Projects in P^{out} to be added to the solution are then selected as in $\mathcal{N}_4$.

Based on a pilot study, the VND algorithm explores the five neighborhoods in the order given in $\mathcal{N}$. A flowchart of the GRASP-VND algorithm is presented in Fig. 2.

6. Experimental analysis

In this section, we perform some computational tests on a set of randomly generated instances to evaluate the efficiency of GRASP-VND in solving FMP instances. The instances were generated by using data provided by TDSI and IMHEN so as to make them as realistic as possible.

6.1. Instance generation

We consider a time horizon $T \in \{10, 20\}$ and two flood scenarios defined by their return period of 20 and 100 years. We generate urban networks of two different sizes $|\mathcal{C}| \times |\mathcal{L}|$: 30 × 300 and 50 × 500. The characteristics of catchments, links, projects and flood impacts are generated to mimic the real data provided by the stakeholders. Namely, the area of a catchment is randomly chosen in the range $[3, 40]$. The length D_l and capacity C_l of a link l are randomly generated in the ranges $[10, 500]$ and $[500, 3000]$, respectively. The traffic volume V_l of a link is computed so that $V_l = \sigma C_l$ where σ is a percentage randomly chosen between 30% and 100%. We assume two types of urban road, with a vehicle speed limit equal to 40 km/h or 60 km/h.

The water depth ranges used to produce the flood maps are discretized by using twelve water depths d_w for $w \in \mathcal{W} = \{1, \ldots, 12\}$, where each depth represents the middle point of a water depth range. Namely, we set $D = \{0.05 + 0.10(w-1) : w \in \mathcal{W}\}$. A water level d_w represents the water depth range $(d_w - 0.05, d_w + 0.05]$. So for example, water level $d_1 = 0.05$ is used as a proxy for a water depth between 0 and 10 cm $((0, 0.1])$.

For the generation of the flood maps, we consider two types of catchments: low risk catchments, which are less flooded during flood events, and high risk catchments, which are flooded with a high water depth. The percentages of flooded areas at different water depths at the beginning of the time horizon are randomly chosen in the ranges $[a, b]$ defined in Table 3. As an example, for a low risk catchment and a 20-year return period, the percentage of flooded area is chosen between 0% and 5% (resp. 0% and 4%) for each water level between 0.05 m and 0.75 m (resp. 0.85 m and 1.15 m). Assume that the area of the catchment is 10 km^2 and the randomly generated percentage of flooded area for $d_1 = 0.05$ is 2%. This means that in a flood scenario with a 20-year return period, an area of 0.2 km^2 in the catchment is flooded with a water level between 0 and 10 cm. The percentage of flooded length at the beginning of the time horizon is computed in a similar way. In addition, we assume that 20% of the links are non-flooded.

We consider that $|\mathcal{P}| \in \{30, 45, 60\}$ if $|\mathcal{C}| = 30$ and $|\mathcal{P}| \in \{50, 75, 100\}$ if $|\mathcal{C}| = 50$. We generate two types of project: small projects with small impacts and costs between \$500,000 and \$1 million, and big projects with more significant impacts and costs between \$1 million

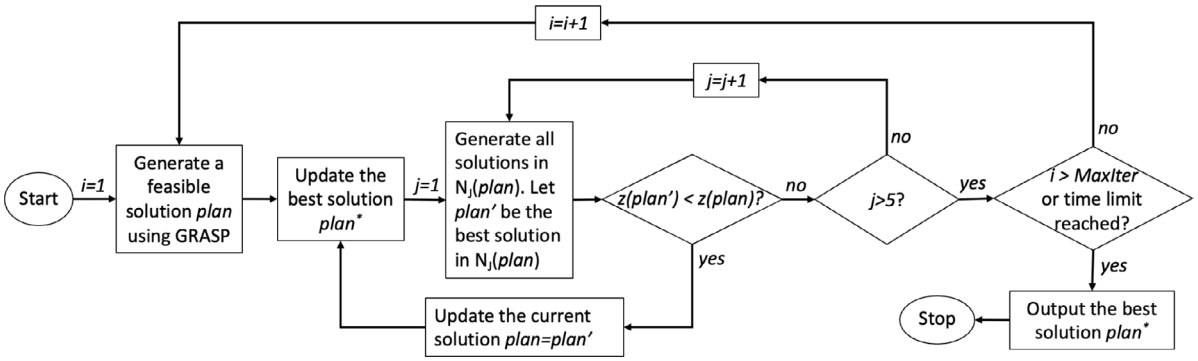

Fig. 2. Flowchart of the GRASP-VND algorithm.

Table 3
Generation of flooded area/length percentages at the beginning of the time horizon.

	Return period	Range (%)	Water level (m)		
			$\{d_1,\dots,d_4\}$	$\{d_5,\dots,d_8\}$	$\{d_9,\dots,d_{12}\}$
Low risk	20	a	0	0	0
		b	5	5	4
	100	a	1	1	3
		b	7	7	6
High risk	20	a	3	3	2
		b	8	8	7
	100	a	5	5	4
		b	11	11	10

Table 4
Generation of the percentage of flooded area and length variation for each project type.

	Return period	Range (%)	Water level (m)		
			$\{d_1,\dots,d_4\}$	$\{d_5,\dots,d_8\}$	$\{d_9,\dots,d_{12}\}$
Small projects	20	a	2	2	5
		b	10	15	20
	100	a	10	10	10
		b	25	30	35
Big projects	20	a	12	12	15
		b	30	35	50
	100	a	20	20	25
		b	45	50	70

and \$3 million. Projects impacts are measured as the percentage of flooded area reduction at each water depth. For each project type, flood scenario and water depth, these percentages are randomly chosen in the range $[a, b]$ defined in Table 4. The percentages of flooded area and flooded length variations are generated in line with the data behind the flood maps produced for Hanoi by IMHEN.

According to the analysis provided by Pregnolato et al. (2017), a vehicle cannot travel when the water level is above 0.3 m. Hence, we set the vehicle speed equal to 1 km/h for water depths equal to 0.35 and above. For the other cases, according to the data provided by TDSI, the vehicles' speeds are set to 22.3 km/h, 18.5 km/h and 9.2 km/h for water depths equal to 0.05 m, 0.15 m and 0.25 m, respectively. The damage rate is computed using the flood depth damage function developed by Kefi et al. (2018) for Hanoi. As recommended by the US Bureau of Public Roads, the parameters of the BPR congestion function are set to $\alpha = 0.15$ and $\beta = 4$.

In the tests, we assume that the total available budget is equal to a percentage B of the total cost of the projects and that the budget is equally spread among the time periods, *i.e.* $B_t = \left(B \sum_{p\in\mathcal{P}} c_p\right)/T$, with $B \in [0, 1]$.

An instance class is characterized by the budget percentage B, the size of the networks $|\mathcal{C}| \times |\mathcal{L}|$ and the number of projects $|\mathcal{P}|$. We generate five instances for each class.

6.2. Analysis

All experiments are performed on a workstation with 128 GB of RAM and two Intel Xeon E5-2680 v3 CPU @ 2.50 GHz, running under the CentOS Linux operating system. The FMP model is solved with IBM ILOG CPLEX 20.1. To avoid memory failures and tune CPLEX performance, we use the following memory setting: the working memory upper limit is set to 64 GB; the node storage file switch parameter is set to 3, so that tree nodes are compressed and written to disk when the working memory limit is exceeded; the upper limit of the branch-and-cut tree size is set to 200 GB. We also set a time limit of five hours. GRASP-VND is implemented in C++. Based on preliminary experiments, the parameter η of the reactive GRASP is chosen in the restricted set $\{0.6, 0.7, 0.8\}$ and the parameter h used in the VND period operators is fixed to 4. The maximum number of iterations *MaxIter* depends on the size of the instances and is set to 150 for the smaller instances ($|T| = 10$ and $|\mathcal{C}| = |\mathcal{P}|$) and to 200 for all the other instances. The maximum running time for the heuristic is set to one hour.

Our initial analysis is performed by giving equal weights to the damage and congestion objectives. Also, equal weights are given to the catchments, time periods and scenarios. Tables 5 and 6 display average statistics on the five instances in each class obtained with CPLEX and GRASP-VND, for $T = 10$ and $T = 20$ respectively. Columns B, $|\mathcal{C}|$ and $|\mathcal{P}|$ display the budget level as a percentage of the total budget, the number of catchments and the number of projects. To evaluate the performance of the algorithms, the percentage gap from the Best Known Value (BKV) is displayed in the columns Gap *BKV* for each approach. BKV is the minimum objective value obtained by either CPLEX or GRASP-VND. Columns Gap *LB* display the percentage gap computed with the formula $(Obj - LB)/LB \times 100$ where Obj is the objective value found by each method and LB is the lower bound found by CPLEX. Columns *Time* indicate the average running time (in seconds) of the algorithms, whereas columns *#BKV* display the number of BKVs found by each algorithm for each instance class. For the GRASP-VND algorithm, the average number of iterations needed to find the solution is reported in the column *#iter*.

Note that CPLEX could not find the optimal solutions in 56 cases for the instances with $|T| = 10$ and in 74 cases for the instances with $|T| = 20$, due to the time or memory limits. Also, in three cases, CPLEX reported the optimal solutions, when in fact the solutions were found to be suboptimal. This is due to CPLEX's precision and truncation errors when dealing with small fractional numbers in the model constraints. Similar issues have been reported in other studies (Berman et al., 2007; O'Hanley et al., 2013).

The results in Tables 5 and 6 show that GRASP-VND outperforms CPLEX, especially for the most difficult instance classes where the

Table 5
Comparison between CPLEX and GRASP-VND for $T = 10$.

B	$\|C\|$	$\|\mathcal{P}\|$	CPLEX				GRASP-VND				
			Average			#BKV	Average				#BKV
			Gap BKV (%)	Gap LB (%)	Time (s)		Gap BKV (%)	Gap LB (%)	Time (s)	#iter	
20	30	30	0.000	0.000	13	5	0.000	0.000	15	11	5
		45	0.003	0.020	5445	4	0.000	0.017	38	23	5
		60	0.005	0.231	18 206	4	0.000	0.226	73	27	4
	50	50	0.000	0.000	484	5	0.000	0.000	104	7	5
		75	0.006	0.092	17 279	2	0.001	0.086	388	86	4
		100	0.116	1.450	18 116	0	0.000	1.332	823	87	5
50	30	30	0.000	0.000	258	5	0.000	0.000	57	33	5
		45	0.026	0.120	18 175	3	0.002	0.096	187	26	3
		60	0.010	1.460	18 087	3	0.006	1.456	456	136	3
	50	50	0.000	0.000	670	4	0.002	0.003	581	31	4
		75	0.004	0.251	18 073	4	0.002	0.249	2540	79	2
		100	0.167	2.853	18 039	0	0.000	2.681	3612	58	5
80	30	30	0.000	0.000	101	5	0.000	0.000	102	56	5
		45	0.115	0.096	18 163	0	0.000	−0.019	395	43	5
		60	0.235	1.633	18 155	0	0.000	1.395	1040	70	5
	50	50	0.000	0.000	5946	5	0.001	0.001	1324	55	3
		75	0.107	0.509	17 136	0	0.000	0.401	3621	40	5
		100	1.085	3.163	18 068	0	0.000	2.055	3664	17	5
Average			0.104	0.660	11 690		0.001	0.554	1057	49	

Table 6
Comparison between CPLEX and GRASP-VND for $T = 20$.

B	$\|C\|$	$\|\mathcal{P}\|$	CPLEX				GRASP-VND				
			Average			#BKV	Average				#BKV
			Gap BKV (%)	Gap LB (%)	Time (s)		Gap BKV (%)	Gap LB (%)	Time (s)	#iter	
20	30	30	0.000	0.000	64	5	0.000	0.000	66	4	5
		45	0.002	0.160	17 725	3	0.000	0.158	115	35	5
		60	0.136	2.326	18 068	0	0.000	2.186	218	87	5
	50	50	0.000	0.000	4159	5	0.001	0.001	284	33	3
		75	0.035	0.794	18 056	0	0.000	0.758	589	83	5
		100	1.104	4.615	18 001	0	0.000	3.473	1032	139	5
50	30	30	0.000	0.013	7414	5	0.001	0.015	219	56	4
		45	0.175	0.489	18 092	0	0.000	0.314	497	103	5
		60	0.232	3.841	18 028	0	0.000	3.600	1148	92	5
	50	50	0.001	0.048	18 070	3	0.003	0.050	1146	133	2
		75	0.087	1.297	18 121	0	0.000	1.208	3217	97	5
		100	1.977	6.556	18 001	0	0.000	4.491	3621	34	5
80	30	30	0.003	0.046	14 041	4	0.001	0.044	344	87	4
		45	0.286	0.720	18 108	0	0.000	0.435	954	119	5
		60	1.401	4.586	18 070	0	0.000	3.140	2521	76	5
	50	50	0.001	0.046	18 138	4	0.007	0.052	2210	97	1
		75	0.225	1.414	18 126	0	0.000	1.187	3634	45	5
		100	2.120	5.836	18 001	0	0.000	3.638	3643	18	5
Average			0.433	1.821	15 460		0.001	1.375	1414	74	

number of projects is strictly greater than the number of catchments. As to be expected, CPLEX seems to perform better on small instances ($|C| = |\mathcal{P}|$). Out of the 90 instances, GRASP-VND finds the best known values for 78 instances when $T = 10$ and for 78 instances when $T = 20$, whereas CPLEX finds it for 49 instances when $T = 10$ and 29 instances when $T = 20$, respectively. GRASP-VND also produces better average gaps, especially on the larger instances with 20 time periods. In terms of time, with the current setting, GRASP-VND noticeably outperforms CPLEX, with the best performance observed on the large instances. As an example, for the most difficult instances with $|\mathcal{B}| = 80$ and $|C| < |\mathcal{P}|$ in Table 6, CPLEX cannot find any BKV after five hours of computing time, whereas GRASP-VND finds all BKVs in less than one hour. For medium instances with $|\mathcal{P}| = 45$, the heuristics finds all the best known solutions in a matter of two to three minutes against the five hours required by CPLEX. Detailed results for a subset of instances ($T = 20$, $B = 20$ and $|C| = 30$) are reported in Table 2 of the supplementary material.

Overall, these results highlight that GRASP-VND is an efficient and effective algorithm for identifying optimal or near-optimal solutions to FMP instances and can be confidently used to generate good approximations of the Pareto front for real instances.

7. Case study of Hanoi, Vietnam

In this section, we provide a practical demonstration of how the proposed approach can be used to support drainage system upgrade decisions in Hanoi.

7.1. Description of the case study

In Hanoi, the capital city of Vietnam, flood risk is very acute. The city has seen increasing urbanization and economic development during recent decades. However, the pace of supportive infrastructure development has lagged behind (Luo et al., 2018), and such pressures are being compounded by more erratic rainfall patterns as a result of

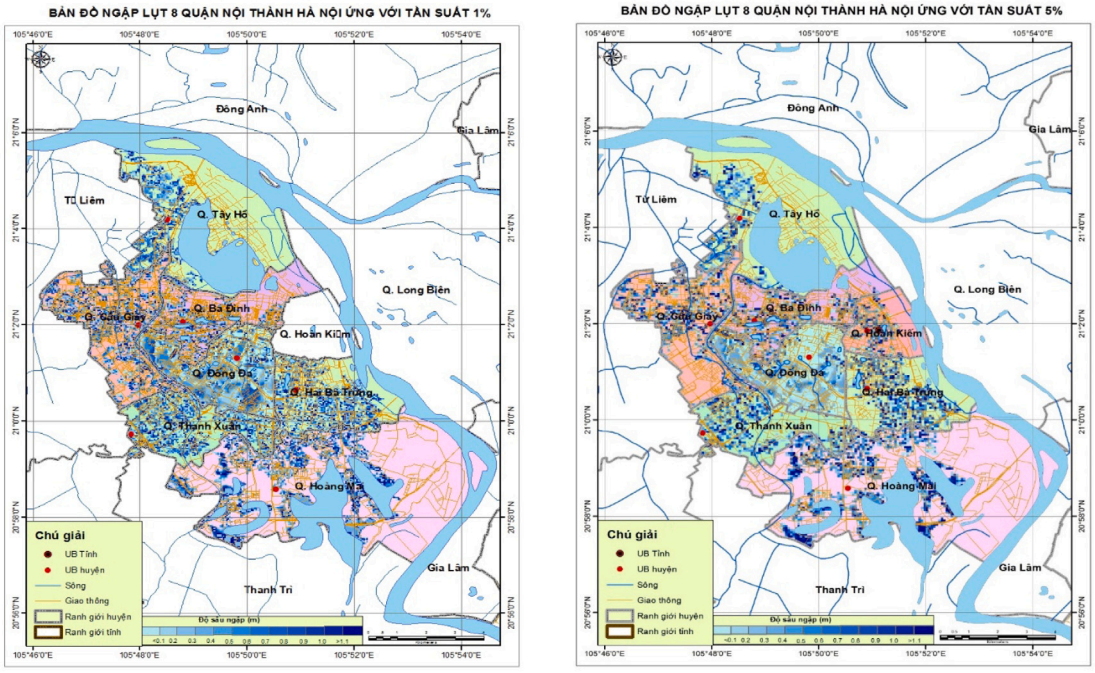

(a) Return period of 100 years. (b) Return period of 20 years.

Fig. 3. Hanoi flood maps in two flood scenarios.

climate change. The city has many hotspots that become waterlogged during heavy rain because of an outdated and overloaded drainage system. In 2008, an historic flood triggered by torrential rain killed 18 people in the city and caused massive economic losses. Urban transportation was halted and food prices reached exorbitant levels as the rain destroyed crops and livestock and crippled transportation corridors (Luo et al., 2018). Following the 2008 flood, the city invested heavily in infrastructural improvements but, in spite of these, it continues to experience serious flooding every year, and the drainage system remains substandard (Hai & Ha, 2022).

The study area considered in this case study includes eight districts in the center of Hanoi: Tay Ho, Ba Dinh, Hoan Kiem, Dong Da, Cau Giay, Hai Ba Trung, Thanh Xuan and Hoang Mai. Based on the flood maps generated by IMHEN (see Fig. 3), the districts were divided into 35 catchments with 377 road segments. The characteristics of the road network (traffic volume, capacity and speed limits) were provided by TDSI.

The impact assessment carried out by AMDI as part of this study revealed that improving the drainage system remains the highest priority to reduce flood risk for local communities in Hanoi (Scaparra et al., 2019). We therefore applied our modeling approach to the central districts of Hanoi, considering a list of potential drainage projects identified through the investment programme review. The initial list included 25 projects, extrapolated from a larger set of about 77 projects listed in the Drainage System Master Plan 2030–2050. These were used by IMHEN to modify the parameters of the drainage system within the MIKE URBAN hydrological model and produce new flood maps of Hanoi under different flood scenarios. The simulated water depths, used as input data for the flood maps, were used to compute the flooded area variations in each catchment and the flooded length variations on the network links. Note that as mentioned in Section 4, the impacts on the water depth reduction of projects in the same catchment are not additive. Therefore, to compute accurate estimates of flooded areas and flooded link lengths, IMHEN generated distinct flood maps for each combination $\mathcal{G}_q$ of projects in the same catchment. A preliminary analysis of the flood maps indicated that the water depth variations induced by some projects were negligible. In addition, one of the projects was already underway at the time of this study. These projects were therefore disregarded and the subsequent analysis was carried out with a subset of 20 drainage system projects, whose details are provided in Table 3 of the supplementary material.

7.2. Results and impacts

To provide the stakeholders with a sample of tradeoff solutions, we solved the bi-objective problem using a classic non-inferior set estimation algorithm (Aneja & Nair, 1979; Stidsen et al., 2014), which iteratively solves the parametric FMP problem to identify the supported extreme nondominated points on the Pareto front. These are displayed in Fig. 4 for two budget levels (20% and 80% of the project total costs). Note that the normalized objective values which identify the points on the Pareto front can be used to derive the reduction in damage and congestion corresponding to each solution. As an example, the upper left point in Fig. 4(a) has coordinates (0.8227, 0.6818), which were obtained by dividing the absolute damage and congestion values by $\bar{D}_B$ and $\bar{C}_B$ (damage and congestion without any project). Consequently, the damage reduction corresponding to this point can be computed as $1-0.8227 = 0.1773$ (or 17.73%). Similarly, the congestion reduction is $1-0.6818 = 0.3182$ (or 31.82%). The analysis shows that if the preferred objective is the congestion level (lower right points), the maximum achievable congestion reductions are about 32.7% and 42.5% with a budget level of 20% and 80% respectively. These drop to 31.8% and 41.9% when the damage is preferred (upper left points). Conversely, the maximum damage reductions are 17.7% and 24.2% with a budget level of 20% and 80% respectively. These drop to 16.2% and 22.2% if congestion is prioritized. Overall, the analysis indicates that considerable reductions in both damage and congestion can be achieved, even with a budget of 20%; the reduction in congestion is more significant than the damage reduction; prioritizing one objective has a modest impact on the deterioration of the other objective, with a slightly more pronounced impact noticeable on the damage reduction when congestion is prioritized.

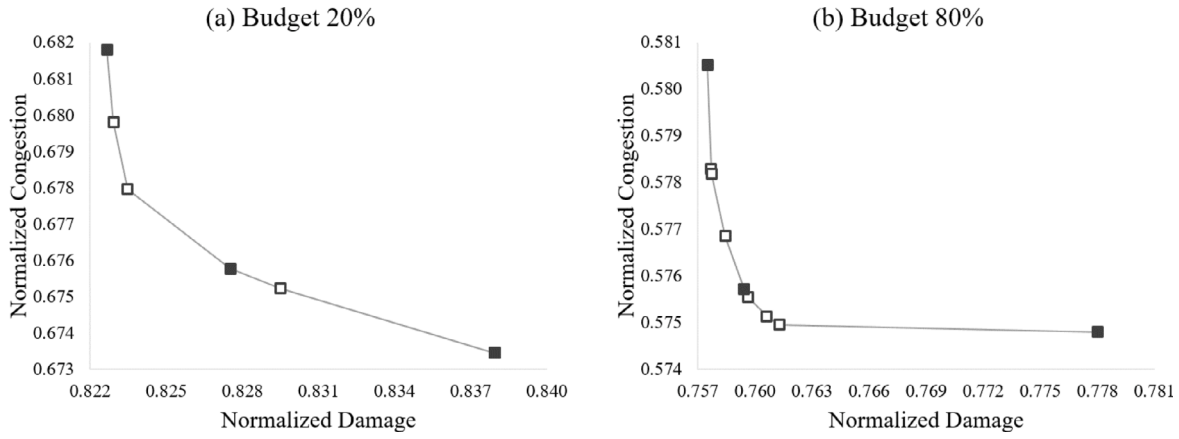

Fig. 4. Trade-off between damage and congestion for two budget levels.

Table 7
Optimal project schedules for three points on the Pareto front and two budget levels.

Periods	Budget 20%			Budget 80%		
	ULP	MP	LRP	ULP	MP	LRP
1	1, 4, 7	1, 4, 7	1, 4, 7	1, 4, 7, 8, 9, 10	1, 3, 4, 6, 7, 8, 10	1, 3, 4, 5, 7, 8, 10
2	9	8	8	3, 13	2, 13	2, 13
3	8	3, 6	3, 5	2, 5, 6, 12	5, 9, 12	6, 12
4	10	10	10	14	14	14
5	2,3,6	2	2	11	11	11
6	5			15	16	16
7						
8		13	13		15	
9	13	5, 9				17
10				18		
11			12			15
12	12	12	6	16	18	
13						
14						
15			14	17	17	18
16	14	14	9			
17						
18	11	11	11			
19						
20				19	20	20
DR (%)	17.7%	17.2%	16.2%	24.2%	24.1%	22.2%
CR (%)	31.8%	32.4%	32.7%	41.9%	42.4%	42.5%

ULP: Upper Left Point; MP: Middle Point; LRP: Lower Right Point.

The solutions corresponding to three points on the Pareto-optimal front (points with solid fill markers) are displayed in Table 7, which shows the selected projects and their implementation period, as well as the overall reduction in damage and congestion for the two budget levels. The optimal schedules show that there are some key projects (1, 4 and 7) which are implemented at the beginning of the planning horizon for each budget level and objective prioritization. The different weights given to the objectives mostly affect the implementation times of the projects. For example, for a 20% budget, project 9, which has more impact on damage reduction than congestion reduction, is delayed from period 2 (ULP) to period 9 (MP) and period 16 (LRP) when more importance is placed on reducing congestion.

Finally, we conducted a sensitivity analysis to the budget level for the case where damage and congestion have equal weights ($\lambda = 0.5$). The results are displayed in Fig. 5, which shows the optimal reduction in damage and congestion obtained with different budget levels for the two flood scenarios and their combination. One of the key findings of the analysis is that more than half of the total reduction in congestion and damage is achieved with less than 20% of the budget, implying that some projects in the current drainage system investment and maintenance programme may not be cost-efficient for mitigating floods. Fig. 5 also shows that for each level of the budget, varying between 0% and 100%, the reduction in both damage and congestion is slightly more significant for floods with a return period of 20 years.

7.3. Graphical user interface

To facilitate the use of the optimization tool by city planners and policy makers, the solution approach is embedded into a Decision Support System (DSS), comprising five main forms. The first three forms enable authorized users to log into the system; select the inputs files, set up some problem parameters (e.g., budget), run the algorithm and visualize the projects' schedule; and obtain some solution statistics (e.g., level of damage and congestion in each district).

The last two forms allow the user to visualize on maps the reduction in damage and congestion after the implementation of the optimized project schedules identified by GRASP-VND. The *Catchment Form* shown in Fig. 6 illustrates the damage in each catchment on color-coded maps, where the colors yellow, orange and red are used to denote low, medium and high damage levels respectively. The map on the left-hand side displays the damage in the base case, while the map on the right-hand side displays the damage after the solution implementation, for a flood with a 100-year return period and a budget equal to 50% of the overall cost of the 20 projects. It can be noted that some red

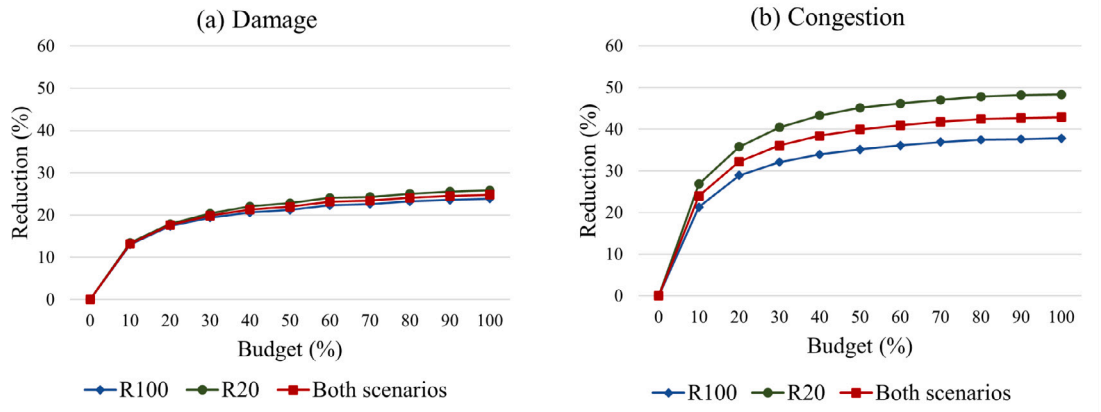

Fig. 5. Trade-off between budget availability and reduction in damage and congestion for 3 scenarios: (i) 100-year return period (R100); (ii) 20-year return period (R20); (iii) a combination of R100 and R20.

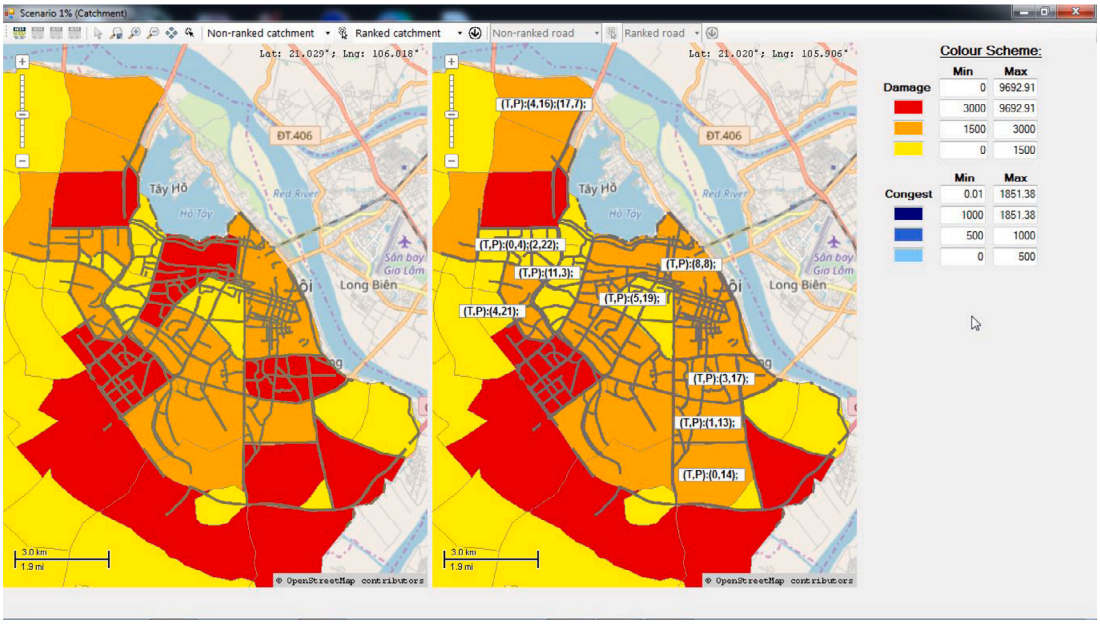

Fig. 6. Catchment Form for Hanoi. (For interpretation of the references to color in this figure legend, the reader is referred to the web version of this article.)

(orange) catchments in the base case (left-hand side map) become orange (yellow) after the projects' implementation (right-hand side map) to denote a significant reduction in damage.

The *Road Form* shown in Fig. 7 illustrates the congestion level on roads before (map on the left) and after (map on the right) the mitigation projects are implemented. Roads are colored using different shades of blue to represent high (dark blue), medium (blue), and low (light blue) congestion levels. As an example, the maps in Fig. 7 show that the level of congestion on two main arteries running from North to South in the Hoang Mai district in the South part of the city is significantly reduced after the project implementation.

Overall, the DSS offers a valuable tool for stakeholders to gain rapid visual insights about the impact on damage and congestion of the recommended solutions in different districts of the city, under different flood scenarios and for different budget levels and objective priorities. Additional details of the DSS and how to use it can be found in the GCRF-OSIRIS DSS user's manual (available at https://research.kent.ac.uk/gcrf-osiris/publications-and-data/).

7.4. Discussion

The pilot study for the city of Hanoi demonstrated the practical applicability of the proposed modeling framework to mitigate urban flood impacts, highlighting both its benefits and limitations. Vietnamese representatives of the Ministry of Transport commended the importance of the research for the twin problems of flooding and traffic congestion in Hanoi. They considered especially important the approach's ability to identify inefficient mitigation measures which had little or no impact on reducing infrastructure damage and congestion. As a result, some of the listed drainage projects were disregarded for future implementation.

Unfortunately, the model could only be tested with 20 projects. This was mostly due to the costs and resources needed to calculate the projects' benefit, which required generating a new flood map using a complex hydraulic model with a modified drainage system for each project combination in the same catchment in each flood scenario. The project team is currently looking to secure funding to test the model

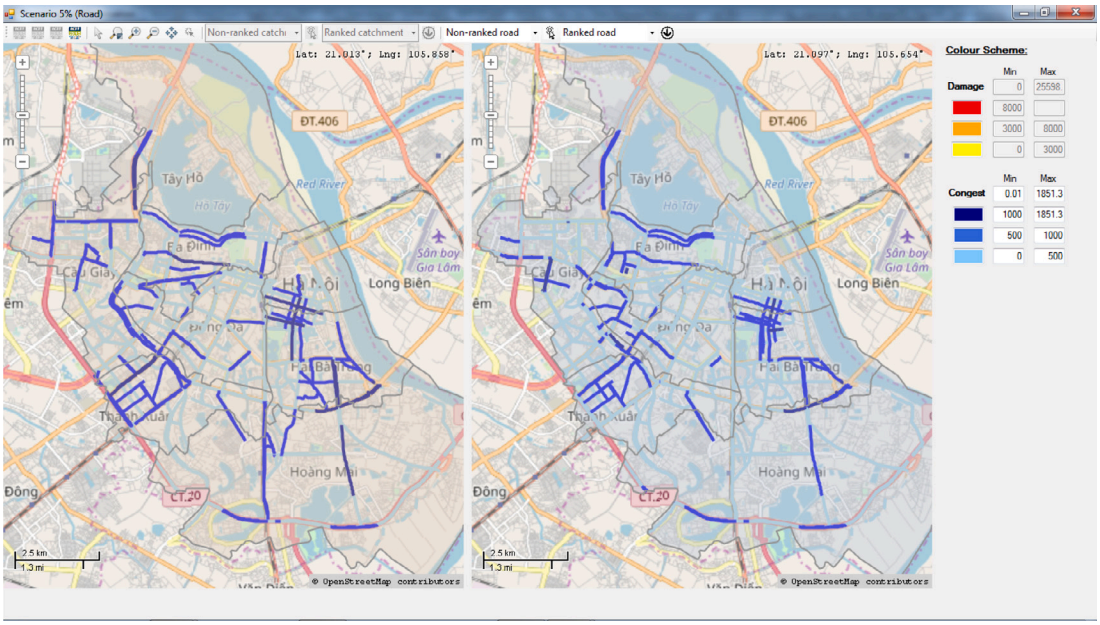

Fig. 7. Road Form for Hanoi. (For interpretation of the references to color in this figure legend, the reader is referred to the web version of this article.)

with additional projects, including projects not originally included in the drainage system master plan, but which were suggested by the IMHEN hydrologists based on the analysis of the flood maps generated in the third project component. The team is also investigating alternative ways of estimating the impacts of multiple interdependent flood defense projects, for example through the use of Artificial Intelligence (AI) methods such as neural network (Dupuits et al., 2019; Mehedi et al., 2022). The development of AI-driven tools to generate flood maps efficiently and rapidly would allow researchers to evaluate dozens of projects and consider additional flood scenarios.

Other limitations of the study which could be addressed in future research to further enhance the model effectiveness and accuracy include: estimating and incorporating costs associated with damage in the model objective; using more sophisticated tools (e.g., microscopic traffic modeling techniques) to model congestion and its cost (He et al., 2021; Pyatkova et al., 2019); more carefully calibrating the timing of the impact of mitigation projects in relation to the duration of their implementation; including discounting in the model to capture the time value of mitigation investments.

In addition, the full model capability should be exploited by experimenting with different prioritization of catchments, flood scenarios and time periods through variations of the model parameters γ_k, β_s and δ_t. As an example, catchments with critical facilities, such as hospitals, may be given higher weights. Also priority could be given to catchments in economically disadvantaged areas, to maximize the reduction of flood impacts among the poor and most vulnerable. By varying the flood scenario weights, different flood mitigation plans can be produced to capture the decision maker risk aversion (e.g., higher priority to most disruptive scenarios).

Although our modeling framework can be applied to other cities, the FMP model was developed specifically to address the needs of the Vietnamese stakeholders and communities. The adaptation to other cities may require considering a variety of flood mitigation measures, both structural and non-structural, and different flood impacts, such as pollution, long-term health effects and damage to cultural heritage. As an example, we are currently investigating a model adaptation for the city of Pakse in Laos where the main objective is to reduce the risk of water-borne viral diseases by improving waste management practices among other measures.

From a methodological point of view, modeling different flood impacts as functions of water depths results in complex multi-objective models which require sophisticated solution techniques to identify representative sets of solutions to be presented to the decision makers. Recent multi-objective optimization studies have focused on generating good representations of the Pareto front which satisfy cardinality, uniformity and coverage criteria (Kidd et al., 2020; Mesquita-Cunha et al., 2023). In our study, we used a simple weighted sum method, which according to Kidd et al. (2020) remains a very competitive method to generate non-dominated points with good coverage of the objective space in reasonable computing time. Future research should be directed to test the adaptability of recent multi-objective MILP solution approaches (Adelgren & Gupte, 2021; Doğan et al., 2022) to solve problems as complex as FMP.

Finally, future modeling efforts should be directed towards capturing the uncertainty characterizing flood disasters in a more robust way. In our study, the uncertainty was captured by using a scenario-based model. However, the practical difficulty of generating flood maps to evaluate projects' benefits in each scenario, limited not only the number of projects we could test, as mentioned earlier, but also the number of scenarios. The use of stochastic optimization or robust optimization techniques should be explored to achieve more robust and effective solutions in the presence of uncertainty related to the frequency, magnitude and impacts of flood events.

In spite of the aforementioned limitations, this study had significant impacts in Vietnam and beyond. Softer areas of impact included increasing connectedness of stakeholders, OR awareness-raising, and momentum for developing an OR culture in Southeast Asia. It has been pointed out in the literature that there is a lack of applications and a lack of collaboration between stakeholders involved in disaster management (Besiou et al., 2018; Çoban et al., 2021). This project enabled stakeholder groups who rarely met to address their common concerns around urban flooding, to start new collaborations and to

appreciate the potential of OR tools to support decision making. Vietnamese institutions involved in the study are now promoting the use of OR to address other sustainable development projects in the region.

8. Concluding remarks

Urban floods pose a serious threat to growing cities in developing countries, undermining their efforts to achieve sustainable development targets. Global discourse on urban flood risk management has highlighted the need to plan and prioritize flood risk reduction investments and to improve stakeholder coordination mechanisms in the planning of mitigation measures (World Bank, 2017). Although donors and humanitarian organizations prioritize investments in short-term response operations, recent studies advocate the need for long-term investments in mitigation, as a way of building sustainability in humanitarian response (Corbett et al., 2022).

In this paper, we developed a comprehensive framework for optimizing flood mitigation investments in Vietnam cities. The Vietnam context provided an opportunity to tackle integrated challenges: working with cross-sectoral stakeholders involved in flood risk management, taking account of interdisciplinary research to create a practical model, and redressing gaps in data and OR DOM applications as identified in previous literature (Gupta et al., 2016).

The core of the framework is a bi-objective optimization model aiming at minimizing road damage and congestion through investments in drainage system projects. The evaluation of the project impacts on damage and congestion required producing flood maps with a modified drainage system for each project and flood scenario. This component of the study involved using advanced meteorological and hydrological models for rainfall simulations and water level estimation in the city catchments. The optimization model objectives were established based on the results of semi-structured interviews conducted by a team of social scientists with members of the local communities. This was to ensure the practical relevance of the proposed model, an aspect which is often neglected in emergency planning studies in the DOM literature (De Vries & Van Wassenhove, 2020). To solve the model efficiently, we developed a GRASP-VND algorithm. Experimental analysis on a set of random instances showed the algorithm's effectiveness in solving realistic problem instances. An important finding of the model application to the city of Hanoi was that using only 20% of the overall project costs would be sufficient to reduce both the damage and congestion rates by half. The analysis also showed that the projects used in the study would be more efficient to reduce congestion than to mitigate damage. Another valuable result for the stakeholders was the identification of inefficiencies in the current drainage system master plan. The generation of flood maps to evaluate the project benefits, in fact, highlighted that some projects in the plan had very limited or no impact in reducing road damage and congestion.

The proposed inter-disciplinary framework has a significant potential to inform flood mitigation planning in many other cities affected by frequent flooding. However, as noted in De Vries and Van Wassenhove (2020), DOM decision making is highly context specific and the context is essential to determine data availability, actors involved, assumptions validity and system constraints. Consequently, generalizability needs to be carefully analyzed, to ensure that optimization models remain relevant to practice. Flood mitigation decisions are no exception. Floods can have a variety of societal impacts that span across space and time (Bubeck et al., 2017), including for example, long-term health effects, damage to cultural heritage and the environment, and most importantly loss of human lives. We argue that adaptations of our modeling framework should reflect local needs and concerns, and take into account a wide range of flood impacts as well as how these are experienced across different groups in society, to ensure fairness and equity in the allocation of flood mitigation resources. We hope that this study will spur future research to address the multi-faceted problem of optimizing flood mitigation efforts in developing countries.

CRediT authorship contribution statement

Siao-Leu Phouratsamay: Conceptualization, Formal analysis, Investigation, Software, Writing – original draft, Writing – review & editing. **Maria Paola Scaparra:** Conceptualization, Formal analysis, Funding acquisition, Methodology, Project administration, Supervision, Writing – original draft, Writing – review & editing. **Trung Hieu Tran:** Data curation, Methodology, Software, Visualization. **Gilbert Laporte:** Methodology, Supervision, Writing – original draft, Writing – review & editing.

Acknowledgments

Thanks are due to two anonymous referees for their valuable and insightful comments. The authors gratefully acknowledge the financial support of the British Academy's Cities and Infrastructure Programme (Ref: CI170099) and of the Engineering and Physical Sciences Research Council, United Kingdom (Ref: EP/T004002/1). The authors also thank all members of the research team at AMDI, IMHEN, TDSI and VAST, the project manager Mr Adutt and the consultant Ms Phuong Dang. Without them, this project would not have been possible.

Appendix A. Supplementary data

Supplementary material related to this article can be found online at https://doi.org/10.1016/j.ejor.2024.06.035.

References

Adelgren, N., & Gupte, A. (2021). Branch-and-bound for biobjective mixed-integer linear programming. *INFORMS Journal on Computing*, *34*(2), 909–933.

ADRC (2022). *Natural disaster databook 2021. An analytical overview*: *Technical report*, Asian Disaster Reduction Center, https://www.adrc.asia/publications/databook/DB2021_e.php. (Accessed November 2023).

Altay, N., & Green, W. G. (2006). OR/MS research in disaster operations management. *European Journal of Operational Research*, *175*(1), 475–493.

Amideo, A. E., Scaparra, M. P., & Kotiadis, K. (2019). Optimising shelter location and evacuation routing operations: The critical issues. *European Journal of Operational Research*, *279*(2), 279–295.

Amin, M. S. R., Tamima, U., & Amador, L. (2020). Towards resilient roads to storm-surge flooding: Case study of Bangladesh. *International Journal of Pavement Engineering*, *21*(1), 63–73.

Aneja, Y. P., & Nair, K. P. K. (1979). Bicriteria transportation problem. *Management Science*, *25*(1), 73–78.

Bangalore, M., Smith, A., & Veldkamp, T. (2019). Exposure to floods, climate change, and poverty in Vietnam. *Economics of Disasters and Climate Change*, *3*(1), 79–99.

Berman, O., Krass, D., & Menezes, M. B. C. (2007). Facility reliability issues in network p-median problems: Strategic centralization and Co-location effects. *Operations Research*, *55*(2), 332–350.

Besiou, M., Pedraza-Martinez, A. J., & Van Wassenhove, L. N. (2018). OR applied to humanitarian operations. *European Journal of Operational Research*, *269*(2), 397–405.

Bhuiyan, T. H., Medal, H. R., & Harun, S. (2020). A stochastic programming model with endogenous and exogenous uncertainty for reliable network design under random disruption. *European Journal of Operational Research*, *285*(2), 670–694.

Brekelmans, R., den Hertog, D., Roos, K., & Eijgenraam, C. (2012). Safe dike heights at minimal costs: The nonhomogeneous case. *Operations Research*, *60*(6), 1342–1355.

Bubeck, P., Otto, A., & Weichselgartner, J. (2017). *Societal impacts of flood hazards*. Oxford Research Encyclopedia of Natural Hazard Science, Oxford University Press.

Caunhye, A. M., Nie, X., & Pokharel, S. (2012). Optimization models in emergency logistics: A literature review. *Socio-Economic Planning Science*, *46*(1), 4–13, Special Issue: Disaster Planning and Logistics: Part 1.

Çelik, M., Ergun, O., Johnson, B., Keskinocak, P., Lorca, A., Pekgün, P., & Swann, J. (2012). Humanitarian logistics. In *New directions in informatics, optimization, logistics, and production* (pp. 18–49). INFORMS.

Choo, K.-S., Kang, D.-H., & Kim, B.-S. (2020). Impact assessment of urban flood on traffic disruption using rainfall–depth–Vehicle speed relationship. *Water*, *12*(4), 926.

Çoban, B., Scaparra, M. P., & O'Hanley, J. R. (2021). Use of OR in earthquake operations management: A review of the literature and roadmap for future research. *International Journal of Disaster Risk Reduction*, *65*, Article 102539.

Corbett, C. J., Pedraza-Martinez, A. J., & Van Wassenhove, L. N. (2022). Sustainable humanitarian operations: An integrated perspective. *Production and Operations Management*, *31*(12), 4393–4406.

CRED (2023). EM-DAT: The emergency events database. www.emdat.be. (Accessed November 2023).

Dang, T.-Q., Phung, C.-D., Nguyen, D.-V., & Dang, P.-L. (2019). *Optimal investment strategies to minimize flood impact on road infrastructure in Vietnam: Technical report*, Vietnam Institute of Meteorology, Hydrology and Climate Change (IMHEN), shorturl.at/ivGLM. (Accessed April 2023).

De Vries, H., & Van Wassenhove, L. N. (2020). Do optimization models for humanitarian operations need a paradigm shift? *Production and Operations Management*, *29*(1), 55–61.

Doğan, I., Lokman, B., & Köksalan, M. (2022). Representing the nondominated set in multi-objective mixed-integer programs. *European Journal of Operational Research*, *296*(3), 804–818.

Dupuits, E. J. C., Klerk, W. J., Schweckendiek, T., & de Bruijn, K. M. (2019). Impact of including interdependencies between multiple riverine flood defences on the economically optimal flood safety levels. *Reliability Engineering & System Safety*, *191*, Article 106475.

Dutta, D., Herath, S., & Musiake, K. (2003). A mathematical model for flood loss estimation. *Journal of Hydrology*, *277*(1), 24–49.

Eijgenraam, C., Brekelmans, R., den Hertog, D., & Roos, K. (2017). Optimal strategies for flood prevention. *Management Science*, *63*(5), 1644–1656.

Eijgenraam, C., Kind, J., Bak, C., Brekelmans, R., den Hertog, D., Duits, M., Roos, K., Vermeer, P., & Kuijken, W. (2014). Economically efficient standards to protect the netherlands against flooding. *INFORMS Journal on Appllied Analytics*, *44*(1), 7–21.

Faturechi, R., & Miller-Hooks, E. (2015). Measuring the performance of transportation infrastructure systems in disasters: A comprehensive review. *Journal of Infrastructure System*, *21*(1), Article 04014025.

Feo, T., & Resende, M. (1995). Greedy randomized adaptive search procedures. *Journal of Global Optimization*, *6*, 109–133.

Galindo, G., & Batta, R. (2013). Review of recent developments in OR/MS research in disaster operations management. *European Journal of Operational Research*, *230*(2), 201–211.

Gao, S. Y., Simchi-Levi, D., Teo, C.-P., & Yan, Z. (2019). Disruption risk mitigation in supply chains: The risk exposure index revisited. *Operations Research*, *67*(3), 831–852.

GFDRR (2015). Country profile: Vietnam. Global Facility for Disaster Reduction and Recovery. https://www.gfdrr.org/en/publication/country-profile-vietnam. (Accessed November 2023).

Grass, E., & Fischer, K. (2016). Two-stage stochastic programming in disaster management: A literature survey. *Surveys in Opererations Research and Management Science*, *21*(2), 85–100.

Gumbel, E. J. (1941). The return period of flood flows. *The Annals of Mathematical Statistics*, *12*(2), 163–190.

Gupta, S., Starr, M. K., Farahani, R. Z., & Matinrad, N. (2016). Disaster management from a POM perspective: Mapping a new domain. *Production and Operations Management*, *25*(10), 1611–1637.

Gutjahr, W. J., & Nolz, P. C. (2016). Multicriteria optimization in humanitarian aid. *European Journal of Operational Research*, *252*(2), 351–366.

Hai, V., & Ha, S. (2022). Long-drawn urban planning issues blamed for hanoi flooding. VNExpress International, https://rb.gy/nmc6x3. (Accessed November 2023).

Hammond, M., Chen, A., Djordjević, S., Butler, D., & Mark, O. (2015). Urban flood impact assessment: A state-of-the-art review. *Urban Water Journal*, *12*(1), 14–29.

Hansen, P., & Mladenović, N. (1999). An introduction to variable neighborhood search. In *Meta-heuristics: advances and trends in local search paradigms for optimization* (pp. 433–458). Boston, MA: Springer US.

Hansen, P., Mladenović, N., Todosijević, R., & Hanafi, S. (2017). Variable neighborhood search: basics and variants. *EURO Journal on Computational Optimization*, *5*, 423–454.

He, Y., Thies, S., Avner, P., & Rentschler, J. (2021). Flood impacts on urban transit and accessibility: A case study of kinshasa. *Transportation Research, Part D (Transport and Environment)*, *96*, Article 102889.

Hien, L. T. K., Sim, M., & Xu, H. (2020). Mitigating interdiction risk with fortification. *Operations Research*, *68*(2), 348–362.

Hoyos, M. C., Morales, R. S., & Akhavan-Tabatabaei, R. (2015). OR models with stochastic components in disaster operations management: A literature survey. *Computers & Industrial Engineering*, *82*, 183–197.

Huizinga, J., Moel, H. D., & Szewczyk, W. (2017). *Global flood depth-damage functions*. Luxembourg: Publications Office of the European Union, http://dx.doi.org/10.2760/16510. (Accessed November 2023).

Huong, H. T. L., & Pathirana, A. (2013). Urbanization and climate change impacts on future urban flooding in Can Tho city, Vietnam. *Hydrology and Earth System Sciences*, *17*(1), 379–394.

Jonkman, S., & Vrijling, J. (2008). Loss of life due to floods. *Journal of Flood Risk Management*, *1*(1), 43–56.

Kefi, M., Mishra, B. K., Kumar, P., Masago, Y., & Fukushi, K. (2018). Assessment of tangible direct flood damage using a spatial analysis approach under the effects of climate change: Case study in an urban watershed in hanoi, Vietnam. *ISPRS International Journal of Geo-Information*, *7*(1).

Kidd, M. P., Lusby, R., & Larsen, J. (2020). Equidistant representations: Connecting coverage and uniformity in discrete biobjective optimization. *Computers & Operations Research*, *117*, Article 104872.

Li, M., Huang, Q., Wang, L., Yin, J., & Wang, J. (2018). Modeling the traffic disruption caused by pluvial flash flood on intra-urban road network. *Transactions in GIS*, *22*.

Luo, P., Mu, D., Xue, H., Ngo-Duc, T., Dang-Dinh, K., Takara, K., Nover, D., & G., S. (2018). Flood inundation assessment for the Hanoi Central Area, Vietnam under historical and extreme rainfall conditions. *Scientific Reports*, *8*, 1–11.

Mehedi, M., Smith, V., Hosseiny, H., & Jiao, X. (2022). Unraveling the complexities of urban fluvial flood hydraulics through AI.. *Science Report*, *12*, 18738.

Mesquita-Cunha, M., Figueira, J. R., & Barbosa-Póvoa, A. P. (2023). New epsilon-constraint methods for multi-objective integer linear programming: A Pareto front representation approach. *European Journal of Operational Research*, *306*(1), 286–307.

Narloch, U., & Bangalore, M. (2018). The multifaceted relationship between environmental risks and poverty: new insights from Vietnam. *Environment and Development Economics*, *23*(3), 298–327.

O'Hanley, J. R., Scaparra, M. P., & García, S. (2013). Probability chains: A general linearization technique for modeling reliability in facility location and related problems. *European Journal of Operational Research*, *230*(1), 63–75.

Özdamar, L., & Ertem, M. A. (2015). Models, solutions and enabling technologies in humanitarian logistics. *European Journal of Operational Research*, *244*(1), 55–65.

Postek, K., den Hertog, D., Kind, J., & Pustjens, C. (2019). Adjustable robust strategies for flood protection. *Omega*, *82*, 142–154.

Prais, M., & Ribeiro, C. C. (2000). Reactive GRASP: An Application to a Matrix Decomposition Problem in TDMA Traffic Assignment. *INFORMS Journal on Computing*, *12*(3), 164–176.

Pregnolato, M., Ford, A., Wilkinson, S. M., & Dawson, R. J. (2017). The impact of flooding on road transport: A depth-disruption function. *Transportation Research, Part D (Transport and Environment)*, *55*, 67–81.

Pyatkova, K., Chen, A. S., Butler, D., Vojinović, Z., & Djordjević, S. (2019). Assessing the knock-on effects of flooding on road transportation. *Journal of Environmental Management*, *244*, 48–60.

Rentschler, J., de Vries Robbé, S., Braese, J., Nguyen, D. H., van Ledden, M., & Pozueta Mayo, B. (2020). *Resilient shores: Vietnam's coastal development-between opportunity and disaster risk*. World Bank, Washington DC, http://hdl.handle.net/10986/34639. (Accessed November 2023).

Rentschler, J., Salhab, M., & Jafino, B. (2022). Flood exposure and poverty in 188 countries. *Nature Communications*, *13*, 3527.

Scaparra, M. P., Chinh, N. C., Phuong, D. T., & Tran, T. H. (2019). Community perceptions of social, economic and environmental impacts of flooding in central districts of hanoi, Vietnam. *Journal of the British Academy*, *7 (s2)*, 137–154.

Sohn, J. (2006). Evaluating the significance of highway network links under the flood damage: An accessibility approach. *Transportation Research, Part A: Policy and Practice*, *40*(6), 491–506.

Starita, S., & Scaparra, M. P. (2021). Improving supply system reliability against random disruptions: Strategic protection investment. *Journal of the Operational Research Society*, *73*, 1307–1324.

Starita, S., Scaparra, M. P., & O'Hanley, J. R. (2017). A dynamic model for road protection against flooding. *Journal of the Operational Research Society*, *68*(1), 74–88.

Stidsen, T., Andersen, K. A., & Dammann, B. (2014). A branch and bound algorithm for a class of biobjective mixed integer programs. *Management Science*, *60*(4), 1009–1032.

Suarez, P., Anderson, W., Mahal, V., & Lakshmanan, T. (2005). Impacts of flooding and climate change on urban transportation: a systemwide performance assessment of the Boston Metro Area. *Transportation Research, Part D (Transport and Environment)*, *10*(3), 231–244.

Tariq, M., Hoes, O., & Van de Giesen, N. (2014). Development of a risk-based framework to integrate flood insurance. *Journal of Flood Risk Management*, *7*(4), 291–307.

Tellman, B., Sullivan, J. A., Kuhn, C., Kettner, A. J., Doyle, C. S., Brakenridge, G. R., Erickson, T. A., & Slayback, D. A. (2021). Satellite imaging reveals increased proportion of population exposed to floods. *Nature*, *596*, 80–86.

UNDRR (2020). *The human cost of disasters 2000–2019. An overview of the last 20 years*. United Nations Office for Disaster Risk Reduction, https://www.undrr.org/quick/50922. (Accessed November 2023).

United States Bureau of Public Roads (1964). *Traffic assignment manual for application with a large, high speed computer*. Washington, DC: U.S. Department of Commerce.

van Dantzig, D. (1956). Economic decision problems for flood prevention. *Econometrica*, *24*(3), 276–287.

Van Wassenhove, L. N., & Pedraza Martinez, A. J. (2012). Using OR to adapt supply chain management best practices to humanitarian logistics. *International Transactions in Operational Research*, *19*(1–2), 307–322.

Win, S., Zin, W. W., Kawasaki, A., & San, Z. M. L. T. (2018). Establishment of flood damage function models: A case study in the bago river basin, myanmar. *International Journal of Disaster Risk Reduction*, *28*, 688–700.

World Bank (2017). *Technical deep dive on integrated urban flood risk management*. United Nations Office for Disaster Risk Reduction, https://www.gfdrr.org/en/publication/technical-deep-dive-integrated-urban-flood-risk-management. (Accessed November 2023).

Zwaneveld, P., Verweij, G., & van Hoesel, S. (2018). Safe dike heights at minimal costs: An integer programming approach. *European Journal of Operational Research*, *270*(1), 294–301.